Chapter 19
Bio-applications of NIR Spectroscopy

Christian W. Huck

Abstract Near-infrared (NIR) spectroscopy occupies a distinct spot as an investigation tool in bioscience. It gained an ultimate value in several areas of application, e.g., in characterization of plant material, examination of body fluids, exploration of the structure and properties of water and biomolecules in aqueous environment. On the other hand, certain limitations of this technique have been apparent and its full potential seems yet to be unveiled. In recent years, key advancements in technology and methods have pushed the frontier of NIR spectroscopy in bio-applications. Trend-setting studies demonstrated the capacity of NIR spectroscopy to excel in previously unattainable scenarios such as in vivo examination of entire organisms. The advent of miniaturized instrumentation enabled a new spectrum of applications in plant-related research. Advancements in data analytical methods decisively pushed the limit in interpretability of NIR spectra, enabling better understanding of NIR spectral features of biomolecules. These advancements were accompanied by a continuous refinement of established approaches. This chapter discussed the established applications, current developments and future prospects of NIR spectroscopy in broadly understood bio-applications.

Keywords Bio-applications · NIR biospectroscopy · Plant analysis · Biomolecules

19.1 Introduction

Near-infrared (NIR) spectroscopy occupies a particular spot across the field of bioscience. On the one hand, it has become the tool-of-choice in various applications concerning the assessment of bio-related samples, e.g., in medicinal plant analysis or quality control of natural products. On the other hand, in several fields such as in-laboratory bioanalytical research and biomedical diagnosis, it steadily gains in importance and challenges the related techniques such as IR or Raman spectroscopies that are well-established tools therein. Because of several reasons, in the

C. W. Huck (✉)
Institute of Analytical Chemistry and Radiochemistry, CCB-Center for Chemistry and Biomedicine, Leopold-Franzens University, Innrain 80-82, 6020 Innsbruck, Austria
e-mail: Christian.W.Huck@uibk.ac.at

Y. Ozaki et al. (eds.), *Near-Infrared Spectroscopy*,
https://doi.org/10.1007/978-981-15-8648-4_19

past decades, a relatively modest attention has been paid to the potential that NIR spectroscopy is able to bring to the latter field. Recent years have demonstrated that NIR spectroscopy may be used in a number of similar applications concurrently with IR or Raman spectroscopy. To better present the strengths and limitations of the eponymous method, it is useful to briefly summarize the essential similarities and differences existing between these approaches. The chemical specificity of IR or Raman spectra is relatively superior to that of NIR spectra, and they are more straightforward in a direct interpretation. The observed bands are broader because of strong overlapping, reducing the potential for linking the spectra with the structural information. This becomes particularly significant in the case of chemically complex samples of biological origin. However, recent years have witnessed rapid progress in our ability to understand NIR spectra of such samples, with combined use of spectral imaging, novel chemometrics or theoretical methods of spectra calculation [1, 2]. Relevant examples will be discussed in this chapter that demonstrate the progress recently achieved at this direction.

IR and NIR spectroscopy differ significantly in the typical sampling depth, or in other words, the information on the sample is collected from distinctively different sample volumes. This fact has a notable influence, as it is common in bioscience to investigate highly inhomogeneous, often micro-structured samples, such as cells and tissues of either plant or animal origin. For example, the consequences of that difference is well exemplified in medical application, in which the optimal sample thickness for IR transmission measurements conveniently matches the typical configuration of microtomed tissue specimen used in conventional medical diagnosis. However, the absorptivity of organic matter is up to two orders of magnitude lower in NIR than in IR region. Consequently, no useful NIR signal can be obtained from such specimen. On the other hand, this permits NIR radiation to reach deeper and measure the spectrum of the sample beneath its surface. This enables, for instance, sensing the information from beneath human skin or examining entire organisms such as fish embryo. Deep tissue sampling is a key advantage for bioanalytical applications. Moreover, for the same reason, a larger sample volume is permissible in NIR spectroscopy, making it better suited for the analysis of bulk materials essential for bio-related studies (e.g., natural products). Moreover, NIR spectroscopy is relatively better suited for examination of samples with high water content. Measurements in transmission or diffuse reflection mode without sample preparation are more feasible than in IR spectroscopy, which requires attenuated total reflection (ATR) approach is such cases. Compared with Raman, which is suitable for examining moist samples, NIR technique is applicable to specimen with high content of fluorophores; those most typically encountered in bioscience are, e.g., chlorophyll or proteins. Because of that, NIR spectroscopy is easily applicable for examination of plants and plant-related materials, as well as protein-rich samples. Better suitability of the principal features of NIR instrumentation in certain applications may be mentioned. Availability of fiber probes makes in vivo diagnosis easier. Miniaturized instrumentation is readily available for NIR spectroscopy. In contrast, such IR sensors are practically limited to ATR, and their application faces difficulties, e.g., because of the stability

of sampling conditions. Worth mentioning is a relatively well-established functional NIR spectroscopy in medical diagnosis, where it serves the purpose of functional neuroimaging.

19.2 Medicinal Plant Analysis

Most often, the therapeutic and medicinal properties of herbs and plants are related to individual bio-active compounds, and their content affects the general usefulness of a given natural product. The chemical composition and the concentration of the bio-active compounds can be analyzed by NIR spectroscopy. The worldwide trend in using medicinal plant products is permanently increasing. In 2018, the turnover with freely available products from pharmacies was more than 1 billion Euro and that from other sources including online business more than another 1 billion Euro. This trend creates high demand for high throughput, in situ analytical methods capable of fast, non-invasive, simultaneous analysis of chemical and physical parameters in order to ensure quality of the natural medicine. Analytical methodologies based on portable, miniaturized NIR instrumentation are essentially favored for this purpose, as direct assessment and optimization of the cultivation conditions and parameters become possible, e.g., the harvest time. However, this application field remains quite new, and the applicability and performance profiles of handheld NIR devices remain continuously investigated.

Kirchler et al. described in their comprehensive examination the capability of NIR spectroscopy supported with various tools to determine the antioxidative potential and related properties of plant medicine. This trend-setting study proposed a new analytical strategy [3]. The performances of one benchtop and two different types of miniaturized NIR spectrometers were tested and compared for the first time by the determination of the rosmarinic acid (RA) content of dried and powdered *Rosmarinus officinalis*, folium (i.e., Rosmarini folium). The recorded NIR spectra (Fig. 19.1) were utilized in hyphenation with multivariate data analysis (MVA) to calculate partial least squares regression (PLSR) models (Table 19.1). Quality parameters obtained from cross-validation (CV) revealed that the benchtop spectrometer achieved the best result with a R^2 of 0.91 and a RPD of 3.27. Miniaturized NIR spectrometer MicroNIR 2200 showed a satisfying calibration value R^2 of 0.84 and a RPD of 2.46. The analysis performed by miniaturized microPHAZIR, with a R^2 of 0.73 and a RPD of 1.88, was less precise and revealed room for improvements. All recorded spectra of the different devices were additionally studied by two-dimensional correlation spectroscopy (2D-COS; details on this technique are available in Chapter 6 Two-dimensional correlation spectroscopy) analysis; in order to support the performed PLS regression models (Fig. 19.2). Differences in the sensitivity of the spectrometers were visualized by 2D hetero-correlation plots as well. These approaches were found to be helpful to identify discrepancies between microPHAZIR and MicroNIR 2200 compared to the benchtop instrument. With the aim to obtain a better understanding of the factors which determine the analyzed PLS regression models, in this study,

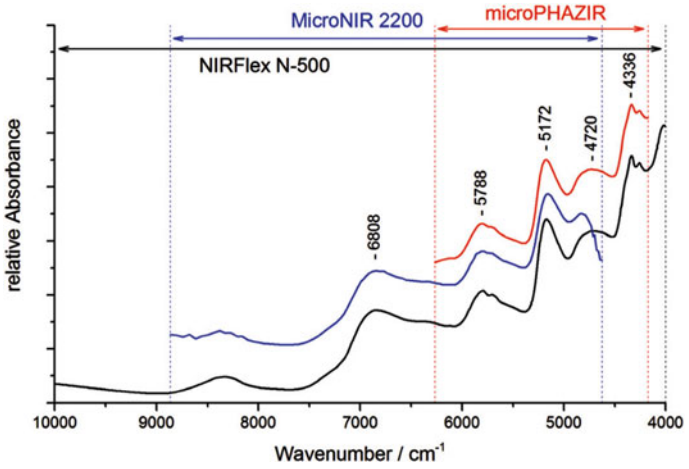

Fig. 19.1 NIR spectra of 60 *Rosmarini folium* samples measured on benchtop (NIRFlex N-500) and two handheld (microPHAZIR and MicroNIR 2200) NIR spectrometers. Reproduced from Ref. [3] with permission from The Royal Society of Chemistry

Table 19.1 Results of all PLSR models for the quantification of rosmarinic acid in *Rosmarinus officinalis, folium*

Spectrometer		NIRFlex N-500		microPHAZIR		MicroNIR 2200	
Samples		60		60		60	
Outliers		6		8		4	
C (w/w) range/%		1.138–2.425		1.138–2.425		1.138–2.425	
Validation method		*CV*	TSV	*CV*	TSV	*CV*	TSV
R^2		*0.91*	0.91	*0.73*	0.73	*0.84*	0.85
SECV/%	SEP/%	*0.072*	0.069	*0.12*	0.11	*0.091*	0.11
SECV/SEC	SEP/SEC	*1.46*	1.43	*1.28*	1.24	*1.55*	2.09
Factors		*8*	8	*5*	5	*11*	12
RPD		*3.27*	3.41	*1.88*	2.06	*2.46*	2.14

quantum chemical calculation of NIR spectrum of RA was carried out. In the process, this approach enabled us to understand, interpret and attribute the main influences in the regression coefficients plots; further information on spectra calculation is given in Sect. 10.8 and in a recent review article [1]. The study by Kirchler et al. demonstrated that the performance of NIR spectroscopy with benchtop and miniaturized devices as a fast and non-invasive technique is able to replace time- and resource-consuming analytical tools [3].

Pezzei et al. compared the suitability of benchtop and portable NIR spectrometers for predicting the optimum harvest time of *Verbena officinalis* [4]. In this project, NIR analyses were performed non-invasively on the fresh plant material based on

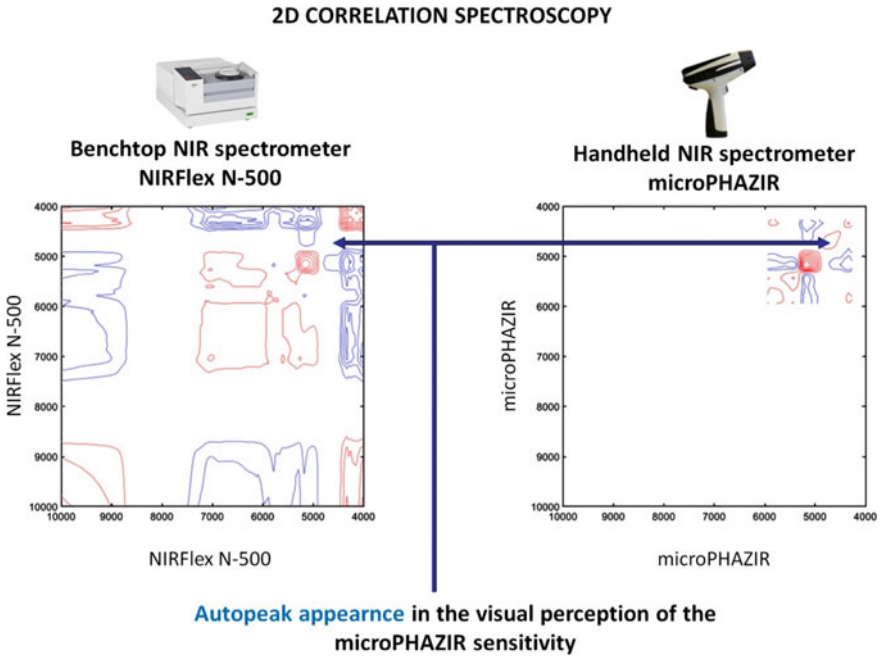

Fig. 19.2 Application of 2D correlation spectroscopy (2D-COS) for the visual assessment and comparison of the sensitivity profiles between different NIR spectrometers; reference benchtop Büchi NIRFlex N-500 vs. handheld Thermo Fisher Scientific microPHAZIR. The comparison of sensitivity: microPHAZIR shows an autopeak located at ca. 4000–5000 cm^{-1} (not observed on the benchtop instrument); this highlights an additional source of spectral variability due to working characteristics of the handheld spectrometer (instrumental nature)

the quantification of the key secondary metabolite ingredients verbenalin and verbascoside. NIR spectroscopic measurements were performed applying a conventional NIR benchtop device as well as a laboratory independent portable NIR spectrometer. A high performance liquid chromatography (HPLC) method served as the reference method. For both instruments, PLSR models were established performing cross-validations (CV) and test-set validations (TSV). Quality parameters obtained for the benchtop device revealed that the newly established NIR method allows sufficient quantifications of the main bio-active compounds of the medicinal plant, verbenalin and verbascoside. Results obtained with the miniaturized NIR spectrometer confirmed that accurate quantitative calibration models could be developed for verbascoside achieving a comparable prediction power to the benchtop instrument. PLS models for verbenalin were less precise suggesting that the application of portable devices may be limited by its spectral range, resolution and sensitivity (Fig. 19.3). Finally, this work demonstrated the suitability of NIR vibrational spectroscopy performing direct measurements on pharmaceutically relevant fresh plant material enabling a quick and easy determination of the ideal harvest time.

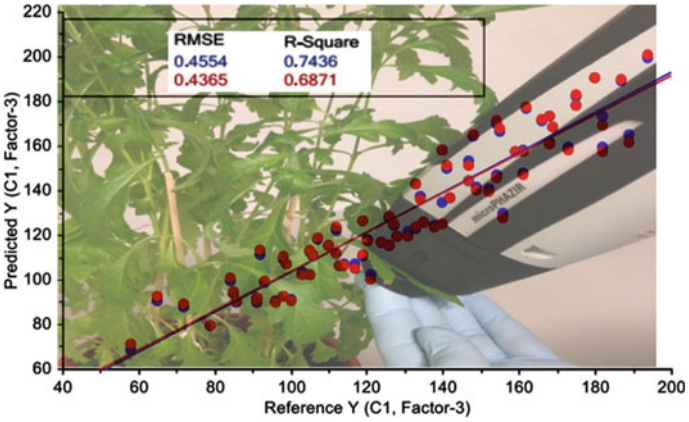

Fig. 19.3 On-site application of portable NIR spectrometer (microPHAZIR) for the optimization of harvest time of medicinal plant *Verbena officinalis*. This is accomplished through PLSR prediction of the content of bio-active compound, verbenalin

Delueg et al. described the online monitoring of the extraction process of Rosmarini folium by an analytical combination of wet chemical assays, UHPLC analysis and a newly developed NIR spectroscopic analysis method [5]. In the stage of experimental design, three different specimen-taking/sampling plans were chosen. At first, monitoring was carried out using three common analytical methods: (a) total hydroxycinnamic derivatives according to the European Pharmacopoeia, (b) total phenolic content according to Folin–Ciocalteu and (c) RA content measured by UHPLC-UV analysis. The combination of the recorded NIR spectra and the previously obtained analytical reference values in conjunction with multivariate data analysis enabled the successful establishment of PLSR models. Coefficients of determination (R^2) were: (a) 0.94, (b) 0.96 and (c) 0.93 (obtained by test-set validation), respectively. Since Pearson correlation analysis revealed that the reference analyses correlated with each other, just one of the PSLR models was required. Therefore, it was suggested that PLSR model (b) be used for monitoring the extraction process of Rosmarini folium. This example demonstrated the potential of NIR spectroscopy in providing a fast and non-invasive alternative analysis method, which can subsequently be implemented for on- or in-line process control in phytopharmaceutical industry.

NIR spectroscopy is a potent tool in qualitative analysis of plants and related samples. For example, the classification, discrimination or authentication of different natural products by the use of NIR spectroscopy is feasible. In particular, classifying the origin of natural products, detecting of adulteration and verifying authenticity of natural products are commonly performed. A considerable utilization this technique has found on the market of traditional Chinese medicines (TCMs). As an example of the applied methodology and achieved accuracy and applicability, Huck-Pezzei et al. established a procedure to discriminate between pharmaceutical formulations

prepared from either *Hypericum perforatum* or *Hypericium hirsutum* originating from China [6]. It has been demonstrated that NIR spectroscopy is capable of discriminating between different plant species, varieties as well as cultivars, plant grown in different conditions or locations. For example, a rapid and accurate discrimination of *Chrysanthemum* varieties using NIR hyperspectral imaging technique (for further details of this technique, reader is referred to the chapter discussing NIR hyperspectral imaging) operating in 11,442–5767 cm^{-1} region (874–1734 nm) was demonstrated by Wu et al. [7]. The examination of the spectral images obtained from 11,038 samples was carried out by means of deep convolutional neural network (DCNN). The study indicated that NIR hyperspectral imaging combined with DCNN is a potent tool for rapid and accurate discrimination of plant varieties. These accomplishments may advance the qualitative analysis useful for producers, consumers and market regulators. Analysis of chemical compositions and various other properties of plants is often the main aim of various applications in agro-food sector. For further information, reader is referred to the chapters focused on this field of application.

19.3 Cell Analysis

IR and Raman spectroscopy have become greatly matured techniques in medical diagnosis of tissues, with prime importance for carcinoma diagnosis. In this field, NIR spectroscopy is still under development, with recent few years marking its significant progress in these applications. For example, its applicability to characterizing breast cancer cells was studied. The behavior of gold nanorods (AuNRs) in metastatic breast cancer cells was investigated by Zhang et al. [8]. The study used absorption spectroscopy in a broad ultraviolet–visible-NIR (UV-Vis-NIR) region (25,000–10,000 cm^{-1}; 400–1000 nm). That case serves an interesting example of how electronic absorption bands that extend to NIR region can be investigated in practical bio-applications (Fig. 19.4). UV-Vis-NIR absorption spectroscopy was employed in combination with inductively coupled plasma mass spectrometry (ICP-MS), transmission electron microscopy (TEM) and dark-field microscopic observation as reference methodologies for examination of the positively charged AuNRs in the highly metastatic tumor cell line MDA-MB-231. Absorption spectra of AuNRs in the living cells were acquired in that study; Fig. 19.4b presents the effects of serum on absorption spectra of AuNRs dispersed in SCM. It was described that characteristic surface plasmon resonance (SPR) peaks of AuNRs can be detected using spectroscopic method with living cells that have taken up the nanorods. The peak area of transverse SPR band was shown to be proportionally related to the amount of AuNRs in the cells determined with ICP-MS. The established spectroscopic analysis method can be used to monitor the behaviors of AuNR. Zhang et al. have demonstrated how successful monitoring the behaviors of AuNRs in the cells can be accomplished through an easy-tu-use UV-Vis-NIR absorption spectroscopic method [8].

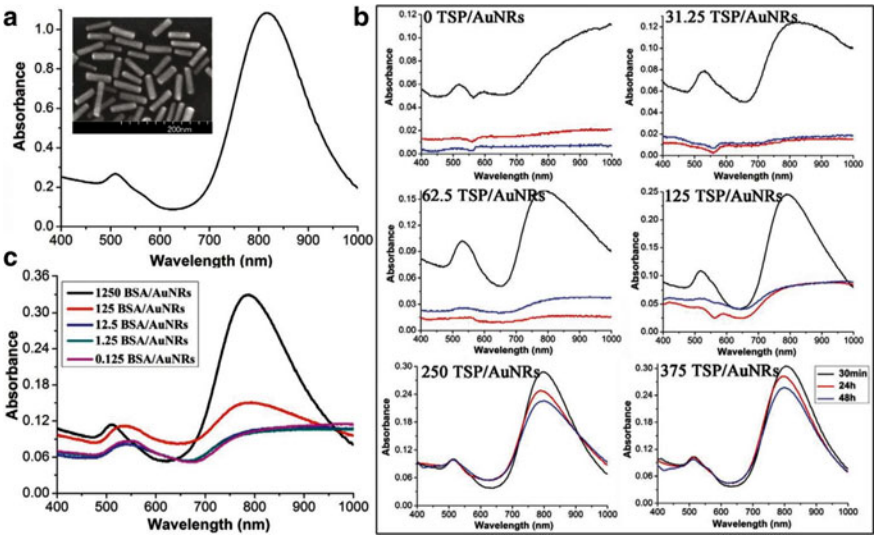

Fig. 19.4 Characterization of AuNRs dispersed in water and culture media. **a** The UV-Vis-NIR absorption spectrum of AuNRs dispersed in water. The inserted SEM image shows the morphology of AuNRs deposited from the aqueous solution. **b** Absorption spectra of AuNRs dispersed in serum containing media (SCM) with 0, 2.5, 5, 10, 20 and 30% of fetal bovine serum (FBS) as a function of incubation time. Concentration of AuNRs in the media was 120 pM. The corresponding ratios of total serum proteins (TSP) to AuNRs (TSP/AuNRs) were 0, 31.25, 62.5, 125, 250 and 375. **c** The absorption spectra of AuNRs dispersed in basic media containing different content of only bovine serum albumin (BSA) for 30 min. The ratios of BSA to AuNRs (BSA/AuNRs) were 1250, 125, 12.5, 1.25 and 0.125. Reproduced in compliance with CC-BY 4.0 license, Ref. [8]

Other examples include similar approaches to prostate cancer cells. In correspondence to carcinoma markers, NIR calibration models for the analysis of glucose, lactate, glutamine and ammonia were established by Rhiel et al., respectively [9]. For the calibration, an adaptive procedure was developed aimed at selective removing metabolism-induced covariance between these analytes arising in the cultivar of PC3-human prostate cancer cells. PLSR models were generated from single-beam NIR spectra recorded between 4800 and 4200 cm^{-1}. Calibration models were in the first attempt developed with both the full spectral range and also with selected optimized spectral ranges. The lowest standard errors of prediction were 0.82, 0.94, 0.55 and 0.76 mM, respectively, for glucose, lactate, glutamine and ammonia. It was demonstrated that NIR spectroscopy can be used effectively in the off-line analysis of glucose and glutamine, as the important nutrients, and lactate and ammonia, as the byproducts, present in a serum-based cell culture medium. Two years later in 2004, the same authors reported about the online monitoring of human prostate cancer cells in a perfusion rotating wall vessel by NIRS [10]. In that study, a perfusion vessel volume, equipped with a silicone membrane oxygenator, peristaltic pump and liquid handling manifold, was installed. For retaining the cells, a 100-μm polypropylene filter was used and separation of cells from other parts was achieved by rotation.

Recording of spectra and establishment of calibration and validation procedures was carried out in the same manner as in the previous contribution published by the same authors [9].

Interestingly, the problem of biological cells appearance in the sample was investigated as a factor potentially influencing the performance of NIR spectroscopy in food analytical applications. For example, Tsenkova et al. examined the influence of high somatic cell count (SCC) in non-homogenized cow milk on the accuracy of NIR spectroscopic determination of fat, protein and lactose content [11]. Transmittance spectra of 258 milk samples were analyzed in SW-NIR, 14,285–9090 cm^{-1} (700–1100 nm) region. The most accurate calibrations, evaluated through analyzing the standard error of prediction and the correlation coefficient, were obtained for the samples with low SCC. The accuracy decreased notably in the scenario, where calibration models constructed on the basis of low SCC milk were used to predict the content of the examined components in samples with high SCC, and vice versa. Therefore, SCC factor is meaningful and highly influences the accuracy of fat, protein and lactose determination. This dependence strongly affects robustness of analysis and needs to be taken into consideration during the determination of milk chemical composition by NIR spectroscopy.

19.4 Serum Analysis

Nioka et al. employed NIR spectroscopy in their approach to test breast tumor-bearing patients who are undergoing a biopsy [12]. The aim was to see if angiogenesis and hypoxia can be used as meaningful factors in detecting cancer. In that attempt, continuous short-wave NIR (SW-NIR) spectroscopy was employed to measure blood hemoglobin concentration and to obtain blood volume. This would allow answering the question, whether the correlated parameters, the total hemoglobin content and oxygen saturation, can serve as the biomarkers for the angiogenesis and hypoxia. Through monitoring these two parameters, high total hemoglobin and hypoxia score, the sensitivity and specificity of cancer detection could be achieved at 60.3% and 85.3% levels, respectively. It was concluded that smaller-size tumors prove to be more challenging for detection by NIR spectroscopy, whereas ductal carcinoma in situ (DCIS) can be detected using configuration assumed in the discussed study. It was noted that in larger-size tumors, there is significantly higher deoxygenation in invasive and ductal carcinoma in situ DCIS than in that of benign tumors [12].

Blood-oxygen-level-dependent contrast functional magnetic resonance imaging (BOLD-fMRI) is a favored tool for detection of brain cancer. However, this technique faces some limitations. The BOLD-fMRI diagnosis in brain disorders such as stroke and brain had been shown in the previous studies to be prone to yield incorrect image activation areas correctly in such cases. Sakatani et al. performed an investigation upon the application of NIR spectroscopy for this purpose [13]. To clarify the characteristics of the cerebral blood oxygenation (CBO) changes occurring in stroke and brain tumors, the authors have been comparing

NIR spectroscopy and BOLD-fMRI recording during functional brain activation in patients. Noteworthy, NIR spectroscopy delivered good diagnostic performances in the cases, in which BOLD-fMRI performed poorly. It was, therefore, concluded that a combined use of both techniques could lead to a higher level of accuracy in the functional imaging of diseased brains [13].

Kasemsumran et al. performed a series of investigations of the analytical capability of NIR spectroscopy in the analysis of human serum albumin (HSA), γ-globulin and glucose for the needs of biomedical purposes. These studies demonstrated the potential for simultaneous determination of HSA, γ-globulin, and glucose by NIR spectroscopy in a model phosphate buffer solution and in a control serum solution that represents a complicated biological fluid [14, 15]. In the study using phosphate buffer solution, five levels of full factorial design were used to prepare a sample set consisting of 125 samples of three component mixtures with various concentrations and examined at 37 °C. The spectral dataset was analyzed using moving-window partial least squares regression (MW-PLSR), which determined the spectral ranges of 4648–4323, 4647–4255 and 4912–4304 cm^{-1} as the most informative and correlated with the content of the targeted molecules (Fig. 19.5) [14]. Subsequently, the analysis of HSA, γ-globulin and glucose in a more complex matrix, the control serum solution, was attempted using an evolutionary chemometric method, searching combination moving window partial least squares (SCMW-PLS). In that study, the control serum IIB (CS IIB) solutions with various concentrations were prepared, and NIR spectroscopy supported by SCMW-PLS was able to successfully determine simultaneously the concentrations of HSA, γ-globulin and glucose in a complex biological fluid [14].

19.5 Saliva Analysis

A diagnostic method based on NIR spectroscopy has been proposed by Murayama et al. for oral cancer detection from one drop of saliva without any specific diagnosis marker [16]. In that study, the NIR spectra of one drop of saliva were measured using a capillary tube method. Principal component analysis with the second and third factors calculated with the second-derivative NIR spectra clearly discriminated between the two groups.

Application of NIR spectroscopy to measurement of hemodynamic signals accompanying stimulated saliva secretion was demonstrated by Sato et al. [17]. That study aimed to explore the feasibility of indirect measurement of human saliva secretion in response to taste stimuli for potential application to organoleptic testing. NIR spectroscopy was used to monitor extracranial hemodynamics, through Hb signals around the temples, of healthy participants upon application of taste stimuli. Functional magnetic resonance imaging (fMRI) was used to provide reference. Statistical analysis indicated that the Hb response and saliva volume are greater upon giving sucrose solution than distilled water to the test group. It was concluded that NIR

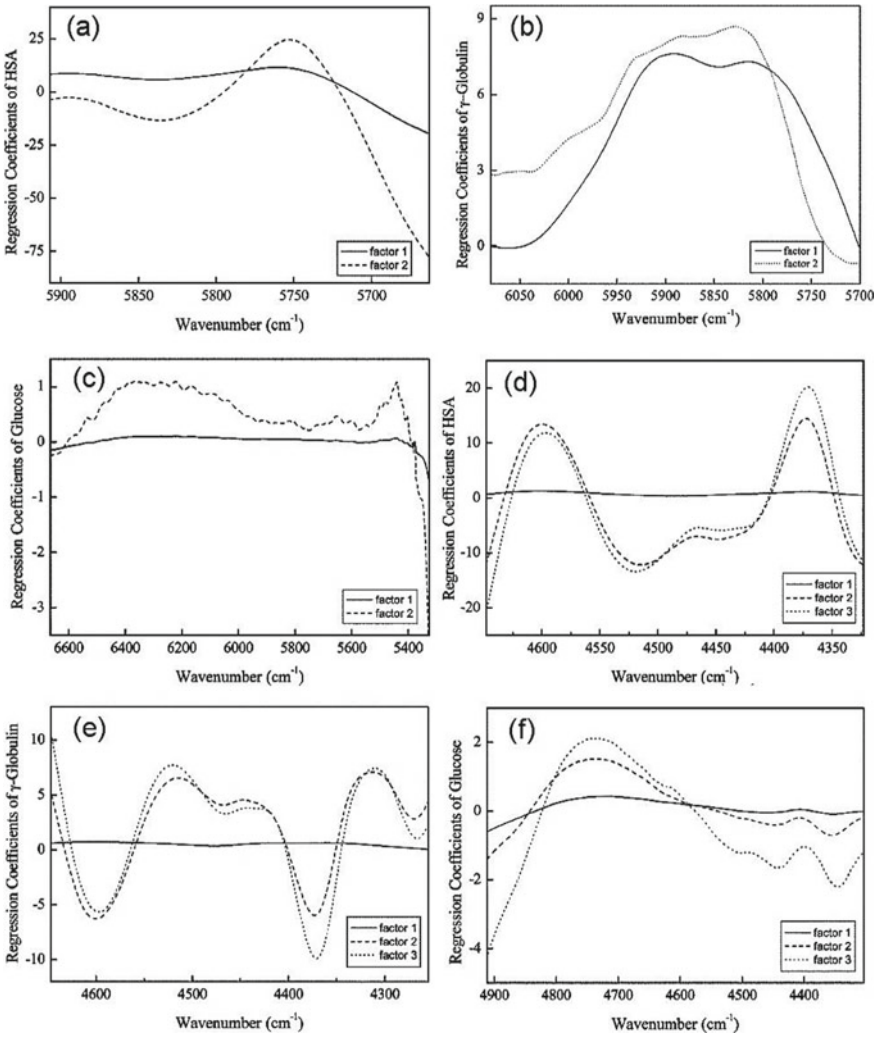

Fig. 19.5 Regression coefficients for the PLS model predicting the analytes concentrations in the study reported by Kasemsumran et al. [Ref. 14]. **a** Factor 1 and factor 2 of HSA in the 5907–5663 cm^{-1} region; **b** factor 1 and factor 2 of γ-globulin in the 6080–5700 cm^{-1} region and **c** factor 1 and factor 2 of glucose in the 6665–5325 cm^{-1}; **d** factor 1, factor 2 and factor 3 of HSA in the 4648–4323 cm^{-1} region; **e** factor 1, factor 2 and factor 3 of γ-globulin in the 4647–4255 cm^{-1} region; **f** factor 1, factor 2 and factor 3 of glucose in the 4912–4304 cm^{-1} region. Reproduced from Ref. [14] with permission from The Royal Chemical Society

spectroscopy is effective in assessing hemodynamic signals accompanying stimulated saliva secretion [17]. NIR spectroscopy appears to be a promising tool for investigation of saliva and processes accompanying swallowing, as this research lane is continuously explored. For instance, recently, Kober and Wood compared the hemodynamic response observed during swallowing of water or saliva using NIR spectroscopy [18]. Relative concentration changes were evidenced in oxygenated and deoxygenated hemoglobin during swallowing. NIR spectroscopy demonstrated high sensitivity to topographical distribution and time course of the hemodynamic response between distinct swallowing tasks. The authors concluded that this approach shows potential for application in diagnostic practice and in supporting therapy for swallowing difficulties [18]. Further examples of the potential that NIR spectroscopy bears in analysis of body fluids are provided in the chapter discussing medicinal applications.

19.6 Tissue Analysis

Tissue analysis is one of the major applications fields of spectroscopy in biomedical sciences. This topic is exhaustively discussed in another chapter of this book that discusses medicinal applications; therefore, only basic information is presented here. For tissue analysis, NIR spectroscopy should be partitioned according to short-wave (SW; 750–1100 nm) and long-wave (LW; 1100–2500 nm) NIR wavelength intervals. At short NIR wavelengths, the hem proteins (hemoglobin, myoglobin and oxy-derivatives) and cytochrome of the tissue dominate the spectra and provide information concerning tissue blood flow, oxygen saturation and consumption, and the redox status of the enzymes. In the LW-NIR region, the observed absorptions are caused by combinations and overtones of vibrations involving hydrogen-containing molecular substructures. Valuable information concerning the chemical composition of the tissue with its main components of lipids, proteins, carbohydrates and water can be gathered from LW-NIR region.

Most of the NIR investigations dealing with human tissues were on breast cancer. Quantitative chemical information from breast tissue based on oxy-hemoglobin and deoxy-hemoglobin, water and lipids has been reported [19]. From these parameters, total hemoglobin concentration and tissue hemoglobin oxygen saturation were calculated and are expected to provide information on tumor angiogenesis and hyper-metabolism.

19.7 Hemodialysis Analysis

Henn et al. described how hemodialysis monitoring can be performed using MIR and NIR spectroscopy with PLSR as the data analytical algorithm [20]. The study aimed to evaluate the feasibility of both techniques and compares their performances. Blood

constituents such as urea, glucose, lactate, phosphate and creatinine are important for monitoring the process of detoxification, especially in ambulant dialysis treatment. Henn et al. compared these two different vibrational spectroscopic techniques to determine the targeted molecules quantitatively in artificial dialysate solutions. The goal of the study was to compare the definitive suitability of NIR and MIR spectroscopy for this purpose. These methods were compared directly by means of statistical errors determined in PLSR analysis, while using the same sample set. Interestingly, Henn et al. presented a detailed analysis of the structure of the PLSR vector developed for quantification of the target analytes in the sample on the basis of MIR and NIR spectra (Fig. 19.6). This comparison demonstrates that relatively

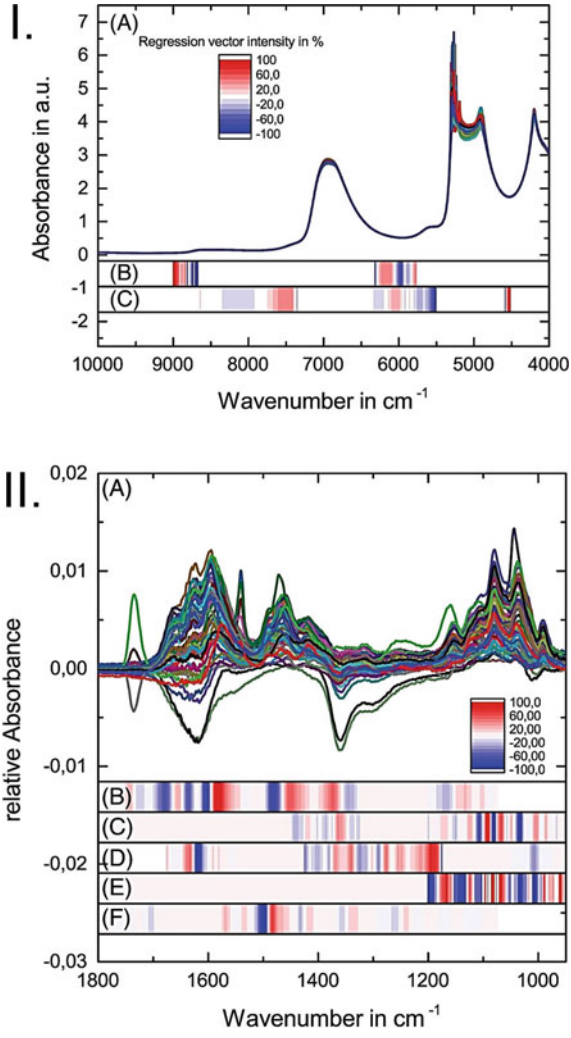

Fig. 19.6 NIR (Panel I) and MIR (Panel II) spectra of the calibration samples used by Henn et al. [Ref. 20]. In Panel I are presented: raw NIR absorbance spectra (**A**); regression vector intensity in percent referenced to the maximum for glucose (**B**) and urea (**C**). In Panel II are presented: raw difference MIR spectra (**A**); the regression vectors in % intensities for urea (**B**), glucose (**C**), lactate (**D**), phosphate (**E**) and creatinine (**F**). Reproduced in compliance with CC-BY 4.0 license, Ref. [20]

few NIR wavenumbers meaningful for regression of glucose and urea concentration in artificial dialysate solutions are found, and these wavenumbers are located in the regions free from a strong absorption of water (Fig. 19.6-I). Multilevel/multifactor design was employed to cover the relevant concentration variations during dialysis. The results demonstrated that MIR spectroscopy is better suited to analyze the molecules of interest. When employed in a multi-reflection ATR mode, it enables reliable prediction of all target analytes. In contrast, the NIR spectroscopic method did not give access to all five components but only to urea and glucose. However, it offered advantages of practical nature, such as easy sampling. For both methods, coefficients of determination R^2 are greater or equal to 0.86, as elaborated in the test-set validation process for urea and glucose. The method applied to the analysis of lactate, phosphate and creatinine performed well in the MIR with $R^2 \geq 0.95$ using test-set validation (Table 19.2). This study indicates that there exists room for improvement in the performance levels of NIR spectroscopy applied to hemodialysis analysis (Table 19.2).

19.8 Examination of Entire Organisms

As mentioned, the underlying physical principles of NIR spectroscopy make it relatively more suitable for interrogation of high-volume samples such as entire biological organisms. As a good example, the properties of fish embryo have recently been comprehensively examined in vivo at the molecular level by Ishigaki et al. [21]. The authors used NIR spectroscopy and imaging for monitoring of the growth of fertilized eggs of Japanese medaka fish. This approach enabled non-destructive examination of the inner components such as proteins, lipids and water, over the 6200–4000 cm^{-1} region. Changes in chemical structure of oil droplets and egg yolk over the time period from the first day after fertilization to the day before hatching were monitored (Fig. 19.7). The study demonstrated that NIR spectroscopy can decipher signs of hatching and metabolic changes in the egg non-invasively. It was revealed that the percentage of strongly hydrogen-bonded water in the oil droplets is larger than in other parts and that yolk has quite different water environments from those found in embryo parts. Furthermore, insights into secondary structure of proteins were obtained. From characteristic bands at 5756 and 4530 cm^{-1} appearance of membrane structures was concluded.

19.9 NIR Studies of the Structure, Properties and Interactions of Biomolecules

Exhaustive presentation of NIR spectroscopy in elucidating information on the molecular structure, properties and interactions is included in Chapter 13 Overview of

Table 19.2 PLSR results for the five-component mixture in dialysate derived from MIR and NIR spectra

Model			Factor	R^2	RMSECV in mg/dL	RMSEP in mg/dL	LOD_{min} in mg/dL	LOD_{max} in mg/dL	LOQ_{min} in mg/dL	LOQ_{max} in mg/dL
Urea	*CV*	*NIR*	*4*	*0.97*	*12*	–	*10*	*24*	*29*	*72*
		MIR	*4*	*0.99*	*7.9*	–	*10*	*18*	*31*	*55*
	TV	NIR	4	0.98	–	19	–	–	–	–
		MIR	5	0.99	–	6.6	–	–	–	–
Glucose	*CV*	*NIR*	*4*	*0.89*	*37*	–	*36*	*73*	*108*	*218*
		MIR	*3*	*0.96*	*22*	–	*47*	*142*	*140*	*428*
	TV	NIR	4	0.86	–	54	–	–	–	–
		MIR	2	0.99	–	11	–	–	–	–
Lactate	*CV*	*NIR*	–	–	–	–	–	–	–	–
		MIR	*5*	*0.95*	*8.2*	–	*28*	90	*84*	*271*
	TV	NIR	–	–	–	–	–	–	–	–
		MIR	8	0.99	3.0	–	–	–	–	–
Phosphate	*CV*	*NIR*	–	–	–	–	–	–	–	–
		MIR	*8*	*0.99*	*1.1*	–	*1.0*	*2.6*	*3.0*	*7.9*
	TV	NIR	–	–	–	–	–	–	–	–
		MIR	8	0.95	–	2.0	–	–	–	–
Creatinine	*CV*	*NIR*	–	–	–	–	–	–	–	–
		MIR	*5*	*0.98*	*1.8*	–	*2.6*	*4.5*	*7.9*	*13*
	TV	NIR	–	–	–	–	–	–	–	–
		MIR	4	0.96	–	2.1	–	–	–	–

– … value not available

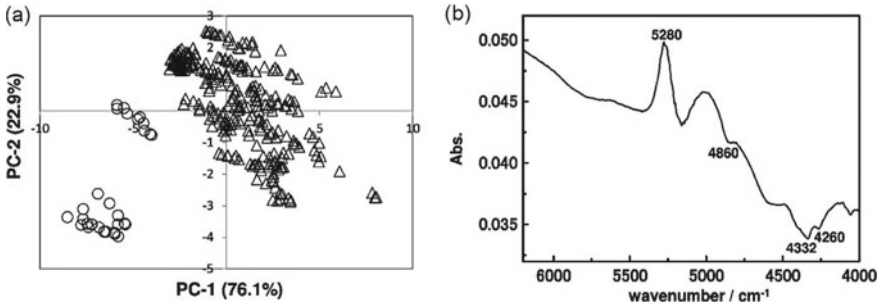

Fig. 19.7 **a** PC-1 and PC-2 PCA scores plot of all NIR spectra of yolk measured over the period from the first day after fertilization until the day before hatching. Δ indicates data from the first to the tenth day and ① denotes data from the day before hatching. **b** Loading plot of PC-1. Reproduced from Ref. [21] in compliance with CC-BY 4.0 license.

application of NIR spectroscopy to physical chemistry; therefore, only brief overview of this field in the context of selected biomolecules is discussed here. Biomolecules are typically complex molecules and they tend to interact with their chemical neighborhood which further complicated their NIR spectra. However, by applying sophisticated methodology, one can obtain valuable information on the behavior of biomolecules. For example, Watanabe et al. employed perturbation-correlation moving-window two-dimensional correlation analysis (PCMW2D) method to monitor the temperature-dependent structural changes in hydrogen bonds occurring in microcrystalline cellulose (MCC) [22]. This approach allowed deducting from NIR and IR spectra that in the temperature range of 25–130 °C, structural changes occur gradually in the strong hydrogen bonds in MCC; the extent of these changes becomes greater above 130 °C. It was concluded that intermediate strength and weak hydrogen bonds arise from the structural changes between 40–90 °C, whereas the appearance of very weak hydrogen bonds becomes dominant above 90 °C. Additionally, PCMW2D correlation analysis enabled band assignments for the first overtone region, and OH groups of MCC exemplifying different hydrogen bonding strength could have been identified. The results of that study enabled further investigations into water adsorption onto MCC [23]. NIR spectroscopy combined with PCMW2D and PCA methods was applied to interrogate a sample set of MCC with the moisture content ranging in 0.2–13.4 wt%. The chosen data analytical methods helped to distinguish OH stretching bands, which heavily overlap in the NIR region due to contributions from MCC and water. Nonetheless, it could have been concluded that a decrease in the free or weakly hydrogen-bonded and an increase in the strong hydrogen-bonded OH groups of MCC occur, with the increase of moisture content. At the same time, an increase of the water adsorbed on MCC was observed. These results suggest that the inter- and intrachain hydrogen bonds of MCC are formed by monomeric water molecule adsorption. The study revealed that ca. 3–7 wt% of adsorbed water is responsible for the stabilization of the hydrogen-bond network in MCC at the cellulose–water surface [23].

NIR spectroscopy is a potent tool in exploring the complex properties of proteins. Protein research by NIR spectroscopy includes several significant contributions, e.g., analysis of the secondary structure [24]. Furthermore, this technique finds unique usefulness in investigating hydration process of proteins. Monitoring changes that occur in hydration as well as that in the protein secondary structure at the same time is possible by NIR spectroscopy; in contrast, IR and Raman spectroscopies can hardly investigate these properties simultaneously. The potential of NIR spectroscopy to investigate proteins in aqueous environment and the appropriate methodology can be presented on the example from literature [25, 26]. Murayama et al. [25] performed a comprehensive comparison of the methods for analyzing NIR spectra that are suitable for investigating proteins in aqueous solution. Conventional spectral analysis methods, chemometrics (PCA) and 2D-COS spectroscopy were evaluated in that case. The study was based on the NIR spectra of human serum albumin (HSA) in aqueous solutions within the concentration range of 0.5–5.0 wt%. It was concluded that basic conventional methods of spectra pretreatment and analysis, such as second-derivative and difference spectra, remain critically important for analysis of protein in relatively low concentration in water. For example, the difference spectra unveiled that various species of water are responsible for the observed gradual concentration-dependent changes in the broad feature in the 7100–6500 cm^{-1}. PCA is more resistant against spectral noise; however, 2D-COS is more informative on the correlations between individual bands and also elucidates sequences of spectral changes. Therefore, the best approach is to combine various methods, as this yields highest potential for interpretation of spectral variability.

With a similar aim, this study has been continued by Yuan et al. who compared different methods for treating NIR spectra of bovine serum albumin (BSA) [26]. However, this time the source of spectral variability was the temperature perturbation (45–85 °C), while concentration of protein was constant at 5.0 wt% and the pH of the sample was 6.8. The evaluated methods were extended by the addition of chemometric algorithm of evolving factor analysis (EFA). That study confirmed the previous conclusions about the usefulness of conventional methods of spectral analysis and the significance of combined use of various approaches. Namely, the difference spectra were essential in finding the change in protein hydration that occurs in the temperature range of 61–65 °C. However, this finding was supported by analyzing the temperature profile through three-factor EFA in the 7400–6400 cm^{-1} region. The investigation has also revealed that the structural variation of BSA in the aqueous solution just precedes the change in the protein hydration, indicating that the change in the hydration is initiated by the structural modifications in the protein itself. For yielding these deeper insights from NIR spectra, application of EFA combined together with the other methods was essential. Note, the spectral variability observed in NIR region upon concentration change of HSA protein in water differs from the one observed upon temperature change in aqueous solution of BSA.

NIR spectral bands of proteins can be used to follow complex biological processes in vivo, such as embryonic development, [27] for example. The current state of the art of protein research by NIR spectroscopy is exhaustively covered in a book chapter by Ishigaki and Ozaki [28]. As mentioned in introduction and in the chapter referred

above, NIR bands can deliver unique information on the properties of such molecules in their native environment. The above examples demonstrate that interpretability of NIR spectra of complex molecules such as biomolecules remains a challenge, and often, only speculative NIR band assignments are available, with selected ones being resolved, e.g., the intense and strongly affected by intermolecular interaction OH stretching bands. Recent advances in quantum chemical calculation of NIR spectra of biomolecules should be highlighted, [1, 29–32] which bring significant progress in the interpretability of their NIR absorption, as well as the insight into how it is influenced by intermolecular interactions. Rapid development of the applicability of these new methods for improving our understanding of NIR spectra of biomolecules should be expected in the near future [1].

19.10 Selected Other Applications

The attributes of NIR spectroscopy have been recognized in ecology and environmental studies. Most often, in such applications, samples of biological origin are investigated. Moreover, spectroscopic analysis is in its essence chemical reagent-free, and as such, spectroscopy itself is environmental friendly. A focused review of the role of NIR spectroscopy in modern research in the field of ecology and environment is available in the recent literature [33].

Over the last few years, entirely, new possibilities have emerged as the result of the progress in unmanned aerial vehicle (UAV, i.e., airborne drones) technology. Such accomplishment became possible on the basis of breakthroughs made in the past decade, with sensor miniaturization, new low-power technology and progress in spectral data processing. There appears an enormous potential from deploying spectroscopic sensors mounted on drones. Applications of airborne NIR sensors installed on UAV are recently strongly advancing in agriculture and environmental studies. Such configuration enables unparalleled high-throughput capability and remote sensing of large Earth surface areas. The current evolution trends are aiming toward real-time monitoring and imaging by using airborne NIR spectrometers. A comprehensive overview of the current state-of-the-art airborne spectroscopy, including NIR, is available in the recent literature [34].

It is worthwhile to mention a narrow field of bio-significant research at which NIR spectroscopy has remarkable accomplishments; investigation of water structure and properties. While not an organic matter, water is an essential biological environment and its properties as well as interactions with other molecules, and biomolecules in particular, are critical for our understanding of biological processes. At this direction, NIR spectroscopy delivered unique insights. Noteworthy is the pioneering research by Segtnan et al. on the structure of water (Fig. 19.8), [35] and combined studies of NIR and IR spectra have also been carried out [36]. Notably, water absorption is comparatively weaker in NIR region than IR region, and simultaneous observation of

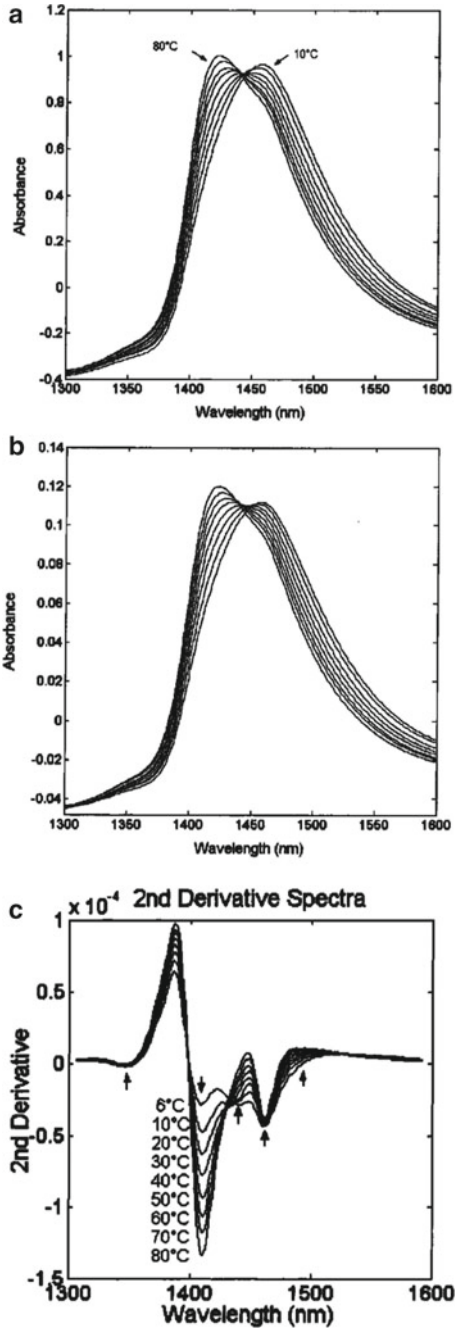

Fig. 19.8 Effect of temperature perturbation of water observed in the NIR spectra by Segtnan et al. [35]. Thirty-eight NIR spectra of water measured over a temperature range of 6–80 °C at 2 °C increments: **a** untreated spectra; **b** mean normalized spectra; **c** selected second-derivative spectra derived from B. Adopted with permission from Ref. [35]. Copyright (2001) American Chemical Society

the characteristic bands of the solvent and soluted molecules is possible. A comprehensive review of the NIR research on water structure and properties is available in the recent literature [37].

A novel way of interpretation of the complex NIR spectra of biomolecules is available through quantum chemical calculation [1]. A comprehensive presentation of this topic is available in Chapter 5 of this book, Introduction to Quantum Vibrational Spectroscopy; therefore, accomplishments essential to further development of bio-applications of NIR spectroscopy are highlighted here. Recently, NIR spectra of several biomolecules such as short-, [29] medium-, [30] and long-chain [31] fatty acids, as well as nucleic acid bases, [32] were successfully reproduced with these methods and their absorption bands could have been comprehensively explained by Beć, Grabska and co-workers [1, 29–32]. This approach was also helpful in interpreting the meaningful wavenumbers in PLSR model of bio-active compounds in plant medicines. Few important bio-active constituents of medicinal plants and natural products have been examined by this approach, e.g., thymol [38] and RA [3]. The studies of thymol supported by spectra simulation yielded fundamental findings about the relationship between the specific vibrational modes and the features of PLS regression coefficients vector [38]. This approach is essential for improving the inherently inferior chemical specificity, which is one of the few properties of NIR spectroscopy at which it exemplifies a great room for improvements in comparison with IR or Raman spectroscopy.

19.11 Conclusions

NIR spectroscopy in the bio-fields offers a huge potential in various applications following its advantages: wide applicability to variety of samples, capability of examining moist samples, flexible instrumentation including miniaturized sensors. Accompanied by advanced chemometric data analytical tools, NIR spectroscopy has been proved to be of great value in various bio-scientific investigations. On the other hand, in certain other fields, it is still a developing discipline, with room for improvement as compared with other techniques. For example, in bioanalytical research and medical diagnosis, it still faces strong competition from IR and Raman spectroscopy. However, the recent literature indicates that NIR spectroscopy steadily conquers this demanding field of application. In the near future, additional support might come by quantum chemical simulation of spectra. New achievements accomplished at this field enable improving the interpretability of NIR spectra; shortening the gap between this technique and highly chemical specific IR or Raman spectroscopy. Novel handheld NIR spectrometers are indispensable in on-site examination of medicinal plants with aim to optimize the cultivation conditions and ensure highest quality of natural drugs. Progress in the instrumentation enabled engineering remote NIR sensors as well. Airborne, UAV-mounted NIR spectrometers become increasingly important in environmental monitoring, where, e.g., large amount of data on is collected on flora

and fauna from wide areas. In summary, bio-applications of NIR spectroscopy can be expected to thrive in the forthcoming decade, with continuation of those strongly advancing lanes of research and possibly an appearance of entirely new ones.

References

1. K.B. Beć, C.W. Huck, Breakthrough potential in near-infrared spectroscopy: spectra simulation. A review of recent developments. Front. Chem. **7**, 48 (2019)
2. W. Huck, K.B. Beć (eds.), *Advances in Near Infrared Spectroscopy and Related Computational Methods* (MDPI, Basel, 2020)
3. G. Kirchler, C.K. Pezzei, K.B. Beć, S. Mayr, M. Ishigaki, Y. Ozaki, C. W. Huck, Critical evaluation of spectral information of benchtop vs. portable near-infrared spectrometers: quantum chemistry and two-dimensional correlation spectroscopy for a better understanding of PLS regression models of the rosmarinic acid content in Rosmarini folium, Analyst **142**, 455–464 (2017)
4. K. Pezzei, S.A. Schönbichler, C.G. Kirchler, J. Schmelzer, S. Hussain, V.A. Huck-Pezzei, M. Popp, J. Krolitzek, G.K. Bonn, C.W. Huck, Application of benchtop and portable near-infrared spectrometers for predicting the optimum harvest time of Verbena officinalis. Talanta **169**, 70–76 (2017)
5. S. Delueg, C.G. Kirchler, M. Meischl, Y. Ozaki, M.A. Popp, G.K. Bonn, C.W. Huck, At-line monitoring of the extraction process of rosmarini folium via wet chemical assays, UHPLC analysis, and newly developed near-infrared spectroscopic analysis methods. Molecules **24**, 2480 (2019)
6. V.A. Huck-Pezzei, L.K. Bittner, J.D. Pallua, H. Sonderegger, G. Abel, M. Popp, G.K. Bonn, C.W. Huck, A chromatographic and spectroscopic analytical platform for the characterization of St John's wort extract adulterations. Anal. Methods **5**, 616–628 (2013)
7. N. Wu, C. Zhang, X. Bai, X. Du, X., Y. He, Discrimination of chrysanthemum varieties using hyperspectral imaging combined with a deep convolutional neural network. Molecules **23**, 2831 (2018)
8. W. Zhang, Y. Ji, J. Meng, X. Wu, H. Xu, Probing the behaviors of gold nanorods in metastatic breast cancer cells based on UV-vis-nir absorption spectroscopy. PLoS ONE **7**, e31957 (2012)
9. M.H. Rhiel, M.B. Cohen, D.W. Murhammer, M.A. Arnold, Nondestructive near-infrared spectroscopic measurement of multiple analytes in undiluted samples of serum-based cell culture media. Biotechnol. Bioeng. **77**, 73–82 (2002)
10. M.H. Rhiel, M.B. Cohen, M.A. Arnold, D.W. Murhammer, On-line monitoring of human prostate cancer cells in a perfusion rotating wall vessel by near-infrared spectroscopy. Biotechnol. Bioeng. **86**, 852–861 (2004)
11. R. Tsenkova, S. Atanassova, Y. Ozaki, K. Toyoda, K. Itoh, Near-infrared spectroscopy for biomonitoring: influence of somatic cell count on cow's milk composition analysis. Int. Dairy J. **11**, 779 (2001)
12. S. Nioka, M. Shnall, E. Conant, S.C. Wang, V.B. Reynolds, B.C. Ching, J.H.T. Swan, P.C. Chung, L. Cheng, D. Shieh, Y. Lin, C. Chung, S.H. Tseng, B. Chance, Breast cancer detection of large size to DCIS by hypoxia and angiogenesis using NIRS. Adv. Exp. Med. Biol. **789**, 211–219 (2013)
13. K. Sakatani, Y. Murata, N. Fujiwara, T. Hoshino, S. Nakamura, T. Kano, Y. Katayama, Comparison of blood-oxygen-level–dependent functional magnetic resonance imaging and near-infrared spectroscopy recording during functional brain activation in patients with stroke and brain tumors. J. Biomed Opt. **12**, 062110 (2007)
14. S. Kasemsumran, Y.P. Du, K. Murayama, M. Huehne, Y. Ozaki, Simultaneous determination of human serum albumin, γ-globulin, and glucose in a phosphate buffer solution by near-infrared

spectroscopy with moving window partial least-squares regression. Analyst **128**, 1471–1477 (2003)
15. S. Kasemsumran, Y.P. Du, K. Murayama, M. Huehne, Y. Ozaki, Near-infrared spectroscopic determination of human serum albumin, γ-globulin, and glucose in a control serum solution with searching combination moving window partial least squares. Anal. Chim. Acta **512**, 223–230 (2004)
16. K. Murayama, M. Tomida, Y. Ootake, T. Mizuno, J.-I. Ishimaru, Principal component analysis for diagnosis of oral cancer using capillary near-infrared spectroscopy of onedrop of human saliva. ITE Lett. Batter. New Technol. Med. **6**, 603–606 (2005)
17. H. Sato, A. Obata, Y. Yamamoto, M. Kiguchi, K. Kubota, H. Koizumi, I. Moda, K. Ozaki, T. Yasuhara, A. Maki, Application of near-infrared spectroscopy to measurement of hemodynamic signals accompanying stimulated saliva secretion. J. Biomed. Opt. **16**, 047002 (2011)
18. E. Kober, G. Wood, Hemodynamic signal changes during saliva and water swallowing: a near-infrared spectroscopy study. J. Biomed. Opt. **23**, 015009 (2018)
19. B.J. Tromberg, A. Cerussi, N. Shah, M. Compton, A. Durkin, D. Hsiang, J. Butler, R. Mehta, Imaging in breast cancer: Diffuse optics in breast cancer: detecting tumors in pre-menopausal women and monitoring neoadjuvant chemotherapy. Breast Cancer Res. **7**, 279 (2005)
20. R. Henn, C.G. Kirchler, Z.L. Schirmeister, A. Roth, W. Mäntele, C.W. Huck, Hemodialysis monitoring using mid- and near-infrared spectroscopy with partial least squares regression. J. Biophotonics **11**, 201700365 (2018)
21. M. Ishigaki, S. Kawasaki, D. Ishikawa, Y. Ozaki, Near-infrared spectroscopy and imaging studies of fertilized fish eggs: in vivo monitoring of egg growth at the molecular level. Sci. Rep. **6**, 20066 (2016)
22. Watanabe, S. Morita, Y. Ozaki, Temperature-dependent structural changes in hydrogen bonds in microcrystalline cellulose studied by infrared and near-infrared spectroscopy with perturbation-correlation moving-window two-dimensional correlation analysis. Appl. Spectrosc. **60**, 611–618, (2006)
23. Watanabe, S. Morita, Y. Ozaki, A study on water adsorption onto microcrystalline cellulose by near-infrared spectroscopy with two-dimensional correlation spectroscopy and principal component analysis. Appl. Spectro. **60**, 1054–1061 (2006)
24. K.I. Izutsu, Y. Fujimaki, A. Kuwabara, Y. Hiyama, C. Yomota, N. Aoyagi, Near-infrared analysis of protein secondary structure in aqueous solutions and freeze-dried solids. J. Pharm. Sci. **95**, 781–789 (2006)
25. K. Murayama, B. Czarnik-Matusewicz, Y. Wu, R. Tsenkova, Y. Ozaki, Comparison between conventional spectral analysis methods, chemometrics, and two-dimensional correlation spectroscopy in the analysis of near-infrared spectra of protein. Appl. Spectro. **54**, 978–985 (2000)
26. Yuan, K. Murayama, Y. Wu, R. Tsenkova, X. Dou, S. Era, Y. Ozaki, Temperature-dependent near-infrared spectra of bovine serum albumin in aqueous solutions: spectral analysis by principal component analysis and evolving factor analysis. Appl. Spectro. **57**, 1223–1229 (2003)
27. M. Ishigaki, T. Nishii, P. Puangchit, Y. Yasui, C.W. Huck, Y. Ozaki, Noninvasive, high-speed, near-infrared imaging of the biomolecular distribution and molecular mechanism of embryonic development in fertilized fish eggs. J. Biophotonics **11**, e201700115 (2018)
28. M. Ishigaki, Y. Ozaki, *Near-infrared spectroscopy and imaging in protein research*, in *Vibrational Spectroscopy in Protein Research*, eds. by Y. Ozaki, M. Baranska, B.R. Wood, I. Lednev (Elsevier, 2020)
29. J. Grabska, M. Ishigaki, K.B. Beć, M.J. Wójcik, Y. Ozaki, Structure and near-infrared spectra of saturated and unsaturated carboxylic acids. An insight from anharmonic DFT calculations. J. Phys. Chem. A, **121**, 3437–3451 (2017)
30. J. Grabska, K.B. Beć, M. Ishigaki, M.J. Wójcik, Y. Ozaki, Spectra-structure correlations of saturated and unsaturated medium-chain fatty acids. Near-infrared and anharmonic DFT study of hexanoic acid and sorbic acid. Spectrochim. Acta A **185**, 35–44 (2017)

31. J. Grabska, K.B. Beć, M. Ishigaki, C.W. Huck, Y. Ozaki, NIR spectra simulations by anharmonic DFT-saturated and unsaturated long-chain fatty acids. J. Phys. Chem. B **122**, 6931–6944 (2018)
32. K.B. Beć, J. Grabska, Y. Ozaki, M.A. Czarnecki, C.W. Huck, Simulated NIR spectra as sensitive markers of the structure and interactions in nucleobases. Sci. Rep. **9**, 17398 (2019)
33. K.R. Counsell, C.K. Vance, Recent advances of near infrared spectroscopy in wildlife and ecology studies. NIR News **27**, 29–32 (2016)
34. K.C. Elliot, R. Montgomery, D.B. Resnik, R. Godvin, T. Mudumba, J. Booth, K. Whyte, Drone use for environmental research. IEEE Geosc. Rem. Sen. M. **7**, 106–111 (2019)
35. V.H. Segtnan, S. Šašić, T. Isaksson, Y. Ozaki, Studies on the structure of water using two-dimensional near-infrared correlation spectroscopy and principal component analysis. Anal. Chem. **73**, 3153–3161 (2001)
36. S. Czarnik-Matusewicz, J.P. Pilorz, Hawranek, Temperature-dependent water structural transitions examined by near-IR and mid-IR spectra analyzed by multivariate curve resolution and two-dimensional correlation spectroscopy. Anal. Chim. Acta **544**, 15–25 (2005)
37. J. Muncan, R. Tsenkova, Aquaphotomics—From innovative knowledge to integrative platform in science and technology. Molecules **24**, 2742 (2019)
38. K.B. Beć, J. Grabska, C.G. Kirchler, C.W. Huck, NIR spectra simulation of thymol for better understanding of the spectra forming factors, phase and concentration effects and PLS regression features. J. Mol. Liq. **268**, 895–902 (2018)